Proceedings of the IX Bulgarian-Serbian Astronomical Conference: Astroinformatics (IX BSACA) Sofia, Bulgaria, July 2-4, 2014,
Editors: M. K. Tsvetkov, M. S. Dimitrijević, O. Kounchev, D. Jevremović and K. Tsvetkova
Publ. Astron. Soc. "Rudjer Bošković" No 15, 2015, 107-115

BEHAVIOUR OF THE FLOW ON THE BOUNDARY IN THE SYSTEM DISK-CORONA

KRASIMIRA YANKOVA

Space Research and Technology Institute, Bulgarian Academy of Sciences
E-mail: f7@space.bas.bg

Abstract. Evolution on the boundary in the system disk-corona has been considered. We present the main set of boundary distributions of the basic features of the flow. Also, the influence of the structure on stream in the primary component (the hot advection accretion disk), over the arising on the secondary component and, respectively, the development of the corona, have been analyzed.

1. INTRODUCTION

In series of articles we develop one model connected with interaction of field and plasma in the accretion disc. In earlier we presented global model for the radial structure of disk (Iankova, 2009; Yankova and Filipov, 2010; Yankova and Filipov, 2011), and model for the local structure (Yankova 2012b; Yankova and Filipov, 2010; Yankova and Filipov, 2011), as an adaptation of the model for the conditions of emerging corona (Yankova, 2012a; Yankova, 2013). We present in this work the behaviour of the boundary between an accretion disk and emerging corona.

2. MODEL

Model is based on the fundamental equations of the magneto-hydrodynamics of fluids. The basic equations of MHD of accretion - disk flow are: the continuity equation (Eq. 2.1), equation of motion (Eq. 2.2), equation of the magnetic induction (Eq. 2.3), equation of heat balance (Eq. 2.4) and equation of state (2.5).

$$\frac{\partial \rho}{\partial t} + \nabla .(\rho v) = 0 \qquad \nabla . v = 0 \qquad \nabla . B = 0 \tag{2.1}$$

$$\frac{\partial v}{\partial t} + v . \nabla v = -\frac{1}{\rho} \nabla p - \nabla \Phi + (\frac{B}{4\pi\rho} . \nabla) B + \vartheta \ \nabla^2 v \tag{2.2}$$

$$\frac{\partial B}{\partial t} = \nabla \times (v \times B) + \eta \nabla^2 B \qquad \eta = \frac{c^2}{4\pi \sigma} \tag{2.3}$$

$$\rho T \frac{\partial S}{\partial t} - \frac{\dot{M}}{2\pi r} T \frac{\partial S}{\partial r} = Q^+ - Q^- + Q_{mag} \tag{2.4}$$

$$p = p_r + p_g + p_m \tag{2.5}$$

Here v =(v_r, rΩ, v_z) is velocity of flux; ρ - mass density; B =(B_r, B_φ, B_z) - magnetic field; Φ - gravitational potential; p -pressure; $\vartheta = \alpha v_s H$ - kinematical viscosity; $\eta = \alpha_m v_s H$ - magnetic viscosity; α- viscosity coefficient; α_m- magnetic viscosity coefficient; v_s- sound velocity; H-half thickness of the disc; σ - magnetic turbulent conductivity ; T- temperature; S - entropy; $\dot{M}$ - accretion rate; Q_{adv} - advective term; Q^+ - viscosity dissipation; Q_{mag} - magnetic dissipation; Q^- - radiative cooling; p_r – radiative pressure; p_g – gas pressure; p_m – magnetic pressure.

3. BOUNDARY DISTRIBUTIONS

In this paper we use the results from theoretical 3D-model of the disk, as obtained in Iankova (2005); Yankova (2012c), for description of the processes on the boundary and to get the *correct boundary distributions* Eq. (3.1-3.8):

$$f_1(x,H) = \frac{c_1 + c_3}{(1 - c_{12} - c_{14})^4 x^{212}} \left[1 - (x - x_g)\right] + 1 \tag{3.1}$$

$$f_2(x,H) = (9c_{z10} + 2)(1 - c_{12} - c_{14})(x - 1) + 1 \tag{3.2}$$

$$f_3(x,H)=\frac{c_6}{2}(1-c_{12}-c_{14})^4(x^2-1)x^4+\frac{c_{z7}}{3}(1-c_{12}-c_{14})^2(x^3-1)x^2+$$
$$+\frac{c_5}{4}(1-c_{12}-c_{14})^2(x^2-1)+(c_1+c_3)\left(\frac{1-c_5(1-c_{12}-c_{14})^2}{2(1-c_{12}-c_{14})^2x^{12}}\right)(x-x_g-1)+1 \quad (3.3)$$

$$f_5(x,H)=\frac{1+c_4}{3}(1-c_{12}-c_{14})\left(\frac{1}{x^2}-x\right)+1 \quad (3.4)$$

$$f_6(x,H)=(1-c_{12}-c_{14})^{-2}\left[\begin{array}{ll}3\dfrac{2+\alpha c_{z10}}{4c_8x^{17/2}}(x-x_g-1)+ & \dfrac{\alpha c_{10}}{c_8x^{13/2}}\dfrac{1}{(x-x_g)^2}\\ -\dfrac{2ac_{z10}-1}{c_8x^{15/2}}\dfrac{1}{(x-x_g)}+ & \dfrac{\alpha c_{z10}-1}{c_8x^2}\end{array}\right]-$$
$$-\frac{c_1(1-c_{12}-c_{14})^{-4}}{c_8}\left(\frac{1}{x^8(x-x_8)}-\frac{1}{x^4}\right)+\frac{c_{z9}}{3c_8}\left(\frac{1}{x^3}-1\right)+ \quad (3.5)$$
$$+(1-c_{12}-c_{14})^2\frac{1}{2}\left(\frac{1}{x^2}-x^2\right)$$

(3.6)

$$f_7(x,H)=-(1-c_{12}-c_{14})^{-1}\left[\frac{c_3}{c_1}+\frac{c_3}{2c_1c_4}\right]\left(\frac{1}{x^{12}(x-x_g)}-\frac{1}{x}\right)-$$
$$-\frac{c_3(1-c_{12}-c_{14})^{-1}}{c_4c_1}\left(\frac{x^{12}}{(x-x_g)^2}-\frac{1}{x}\right)-\frac{c_{17}(1-c_{12}-c_{14})^{-3}}{c_1}\left(\frac{1}{x^3}-\frac{1}{x^{32}(x-x_g)}\right)+$$
$$+\frac{5+20c_{z10}}{c_1}(1-c_{12}-c_{14})\left(\frac{1}{x}-x\right)-\frac{4c_{z6}}{c_1}\left(\frac{1}{x}-1\right)$$

$$f_8(x,H)=\left(-\frac{c_4+1}{k_0}-\frac{2c_4}{c_{z6}}\right)(x-1)+\frac{(c_1+c_3)}{c_{z6}(1-c_{12}-c_{14})^2x^{12}}(x-x_g-1)-$$
$$-\frac{k_0^2+2}{2k_0(1-c_{12}-c_{14})^2}\left(1-\frac{1}{x^2}\right)+\frac{c_{z5}}{c_{z6}(1-c_{12}-c_{14})^2}\left(\frac{1}{x}-\frac{1}{x^2}\right)+ \quad (3.7)$$
$$+\frac{1+c_4}{(1-c_{12}-c_{14})}\left(1-\frac{1}{x}\right)$$

(3.8)

$$f_9(x,H) = \frac{c_{z3}}{\left(x - x_g\right)} - \frac{c_{z2}(1 - x^{-2})}{2(1 - c_{12} - c_{14})^2} - \frac{c_{z4}(1 - c_{12} - c_{14})^2}{3}(x^3 - 1)x^2 - c_{Z3} + 1$$

Here $f_1(x,H)$, $f_2(x,H)$, $f_3(x,H)$, $f_5(x,H)$, $f_6(x,H)$, $f_7(x,H)$, $f_8(x,H)$, $f_9(x,H)$, are respectively the dimensionless functions of the boundary distributions on the parameters ρ, $\boldsymbol{v}_r$, $\boldsymbol{v}_s$, $\boldsymbol{B}_r$, $\boldsymbol{B}_\varphi$, $\boldsymbol{v}_z$ of the flow, and the coefficients of meeting ω, k_φ, of the boundary in the system disk-corona. The c_i *and* c_{zi} are dimensionless combinations of parameter values at the outer edge of the disc F_{i0} (given in Appendix).

4. RESULTS

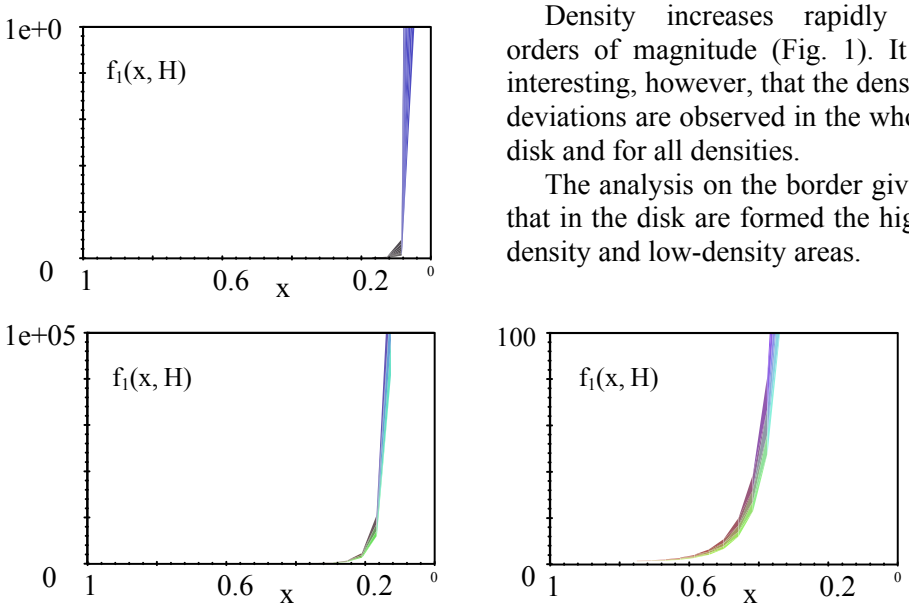

Density increases rapidly in orders of magnitude (Fig. 1). It is interesting, however, that the density deviations are observed in the whole disk and for all densities.

The analysis on the border gives, that in the disk are formed the high-density and low-density areas.

Figure 1: Vertical boundary distributions of the function of the equatorial density.

Equatorial density shows two types of contours. The low-density contours are closed rings. And the high-density contours are open-helices, which follow the angle of the tidal helix (Fig. 2). This can be easily supposed and explained by amenable, movable boundary distributions of the sound and the magneto-sonic speeds (Fig. 3c, d). Mutability of these boundary distributions is caused by the overall interaction between the parameters and the influence of the non-linear effects over them.

These two types of velocities are the most sensitive to the energy exchange and energy distribution in the disk. The mobile maximum and minimum, respectively, create multiple contours of increasing. This behaviour, combined with existing and fast growing magnetic field (Fig. 4) ensure the emergence of compacted regions genetically unrelated to the helices. These are precisely the advective rings that provide heating function of the pad at the base of the corona.

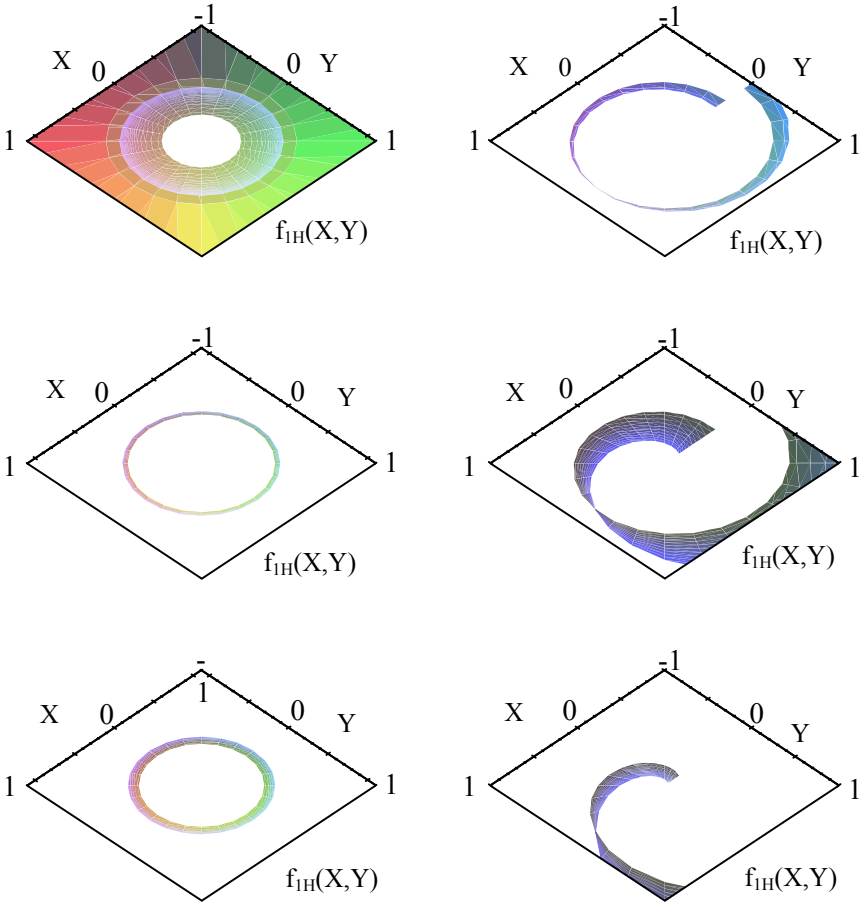

Figure 2: Cylindrical boundary contours of the function of the equatorial density.

The radial and the vertical velocities show typical behaviour along the border (Fig. 3a, b).

Contours of the increase of the radial field (Fig. 5) are not continuous, however, maintains a certain axisymmetry. On one hand, this confirms the presence of the compact regions and on the other, talks about the energy exchange between the components of the field.

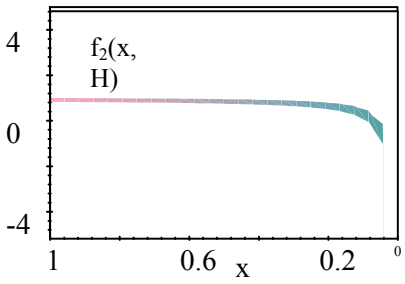

(a) Distribution of the radial velocity.

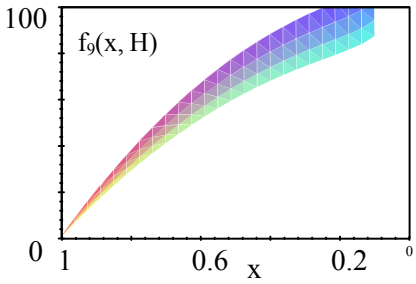

(b) Distribution of the vertical velocity.

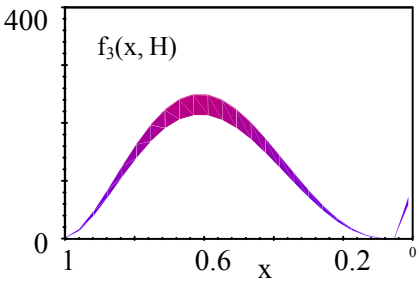

(c) Distribution of the sound velocity.

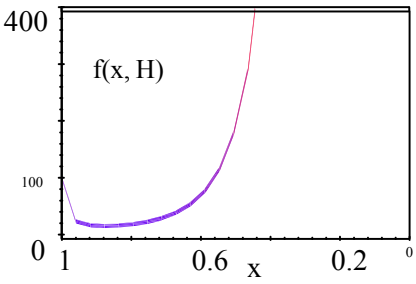

(d) Distribution of the magneto-sonic velocities.

Figure 3: Vertical boundary distributions of the functions of the velocities.

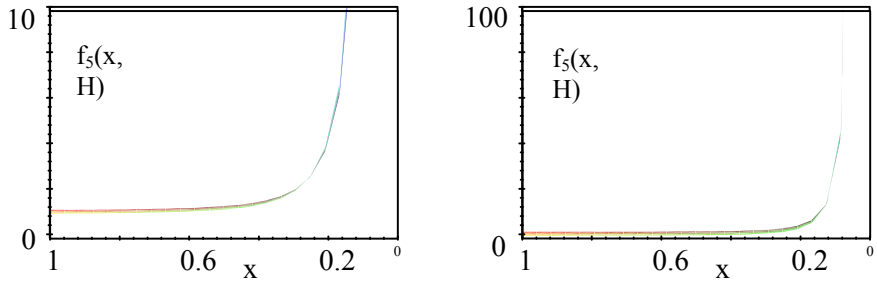

Distributions of the contours of the radial magnetic field.

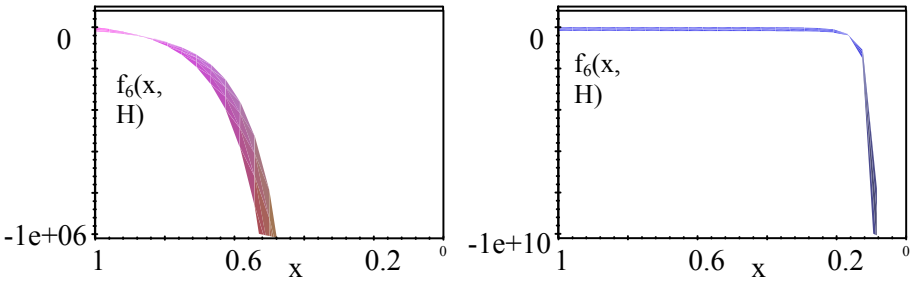

Distributions of the contours of the azimuthal magnetic field.

Figure 4: Vertical boundary distributions of the functions of the magnetic fields.

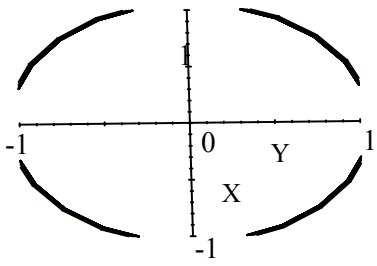

Figure 5: Cylindrical boundary contours of the function of the radial magnetic field.

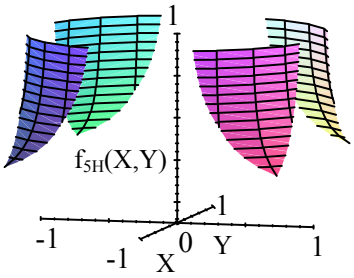

Cylindrical distributions of the boundary function of the radial magnetic field.

5. CONCLUSION

Vertical structure allows correcting the initial distributions $f_i(x, H)$ for the fluid on the boundary disc-corona $f_4(x)$. (On the lower limit of corona such conditions obtained from 2D-structure: $f_i(x, 0)= f_i(x)$ are not suitable because of averaging over z). It complements the 2D-model quality by unfolding descriptive possibilities of the global model as a whole.

Correction is especially important because on the boundary manifest themselves the effects of the warming into the pad:

Tightening of advective rings leads the energy in the form of heat, to the center of the disk. Negative entropy leads to a new state by irreversible conversion and arises corona. The warming into the pad is the major factor that supports the disk's wind and does not allow corona to attenuate (convective coronas shows a cyclic attenuation).

The effect is reinforced by behaviours of the floating extremums of the magneto-sonic and of the sound velocities. They create the necessary environment of the magnetic field to transfer energy between its components - thus creating a permanent instability in the plasma and condition to the self-induction of advection in disk.

These results will allow us in the future when we use the model for real object, to estimate the life cycle of radiative corona that shows such a disc. Also to determine the extent to which the primary component exerts influence on the development of the coronal component of the system.

References

Iankova, Kr. D.: 2005, SSTRI-BAN, SES 2005 proceedings, 30-36.

Iankova, Kr. D.: 2007, 5th Bulgarian-Serbian Conference (V BSCASS): "Astronomy and Space Science", Heron Press Ltd. Science series, pp 326-29. http://aquila.skyarchive.org/5_BSCASS/create/presentations/Iankova.pdf

Iankova, Kr. D.: 2009, Proc. VI Serbian-Bulgarian Astronomical Conference, *Publ. Astr. Soc. "Rudjer Bošković",* **9**, 327-333. http://aquila.skyarchive.org/6_SBAC/pdfs/31.pdf

Yankova, Kr. D.: 2012a, SSTRI-BAN, SENS 2011 proceedings, 73-78. http://www.space.bas.bg/SES2011/Sp-Ph-9.pdf

Yankova, Kr. D.: 2012b, *Publications of the Astronomical Society "Rudjer Boskovic",* **11**, 375-383. http://adsabs.harvard.edu/abs/2012PASRB..11..375Y

Yankova, Kr. D.: 2012c, JUBILEE INTERNATIONAL CONGRESS: SCIENCE, EDUCATION, TECHNOLOGIES "40 YEARS BULGARIA – SPACE COUNTRY ", proceedings, Tom 1, 152-158.

Yankova, Kr. D.: 2013, Proceedings of the VIII Serbian-Bulgarian Astronomical Conference (VIII SBAC), *Publ. Astron. Soc. "Rudjer Bošković",* **12**, 375-381. http://wfpdb.org/ftp/8_SBAC_D1/pdfs/34.pdf

Yankova, Kr., Filipov, L.: 2010, SSTRI-BAN, SENS 2009 proceedings, 370-375.

Yankova, Kr., Filipov, L.: 2011, SSTRI-BAN, SENS 2010 proceedings, 389-394.

APPENDIX

In the table are presented the dimensionless constants in the boundary distributions of the leading parameters of the flow Eq. (3.1-3.8). They were obtained in the process of solving 2D- and 3D-structures of the model on the disk Eq. (3.1-3.8).

$c_1 = \frac{r_0 \omega_0}{v_{r0}}$	$c_2 = \frac{9 v_{s0} H_0}{v_{r0} r_0}$	$c_3 = \frac{\Omega_0 r_0 k_{\phi 0}}{v_{r0}}$
$c_4 = \frac{k_{\phi 0} B_{\phi 0}}{B_{r0}}$	$c_5 = \frac{v_{r0}^2}{v_{s0}^2}$	$c_6 = \frac{k_{\phi 0} B_{\phi 0} B_{r0}}{8 \pi \rho_0 v_{s0}^2}$
$c_7 = \frac{B_{z0} B_{r0} r_0}{8 \pi \rho_0 H_0 v_{s0}^2}$	$c_8 = \frac{B_{r0} B_{\phi 0}}{4 \pi \rho_0 r_0 \Omega_0 v_{r0}}$	$c_9 = \frac{B_{z0} B_{\phi 0}}{4 \pi \rho_0 H_0 \Omega_0 v_{r0}}$
$c_{10} = \frac{v_{s0} H_0}{v_{r0} r_0}$	$c_{11} = \frac{2 v_{s0} r_0}{v_{r0} H_0}$	$c_{12} = \frac{2 \rho_0 v_{s0}^2}{3 B_{z0} B_{r0}}$
$c_{13} = c_{10} k_{\phi 0}$ $c_{16} = c_{10} k_{\phi 0}^2$	$c_{14} = \frac{2 \rho_0 r_0^2 \Omega_0^2}{3 B_{z0} B_{r0}}$	$c_{15} = \frac{r_0 B_{z0}}{H_0 B_{r0}}$
$c_{17} = \frac{\Omega_0 r_0^2 B_{z0}}{v_{r0} H_0 B_{\phi 0}}$	$c_{z1} = \frac{v_{z0}}{v_{r0}}$	$c_{z2} = \frac{v_{s0}^2}{v_{r0} v_{z0}}$
$c_{z3} = \frac{\Omega_0^2 r_0^2}{v_{r0} v_{z0}}$	$c_{z4} = \frac{3 B_{z0} B_{r0}}{4 \pi \rho_0 v_{r0} v_{z0}}$	$c_{z5} = \frac{B_{z0}}{B_{r0}}$
$c_{z6} = c_{z10} k_{\phi 0}$	$c_{z7} = \frac{B_{z0} B_{r0}}{8 \pi \rho_0 v_{s0}^2}$	$c_{z9} = \frac{B_{z0} B_{\phi 0}}{4 \pi \rho_0 v_{r0} \Omega_0 r_0}$
$c_{z10} = \frac{v_{s0}}{v_{r0}}$	$c_{z16} = \frac{k_{\phi 0} v_{s0} B_{r0}}{v_{r0} B_{\phi 0}}$	$c_{z17} = \frac{\Omega_0 r_0 B_{z0}}{v_{r0} B_{\phi 0}}$

The constants here are dimensionless combinations of initial values of the leading parameters on the outer edge of the disk: r_0- outer radius; v_{r0} is the initial radial velocity of flux; Ω_0- initial angular velocity; v_{z0}- initial vertical velocity; v_{s0}- initial sound velocity; H_0- initial half thickness of the disc; ρ_0 – initial equatorial mass density; B_{r0} $B_{\varphi 0}$ B_{z0} – components magnetic field; ω_0- and $k_{\varphi 0}$- the coefficients of meeting, too.